

## Enrichment Measurement of Nuclear Materials by Passive Gamma-ray Analysis

Jong Sook Hong, Hong Ryul Cha, Hyoung Nae Choi,  
Byung Doo Lee and Ho Joon Park

Korea Atomic Energy Research Institute

(Received August 23, 1990)

### 수동적 감마선분석에 의한 핵물질 농축도 측정

홍종숙 · 차홍렬 · 최형내 · 이병두 · 박호준

한국원자력연구소

(1990. 8. 23 접수)

### Abstract

U-235 enrichment has been measured non-destructively by passive gamma-ray pulse height analysis. Measurement source is 185.7 keV gamma-ray which is emitted from uranium sample during alpha decay of U-235 in it. Factors influencing the measurement such as sample composition, attenuation effect of container wall, collimation effect and counting efficiency were evaluated. Under the optimized counting system, the measured relative errors were ~8%, ~8% and ~1% from Tag values at 95% confidence level for depleted UF<sub>6</sub> cylinders, depleted UO<sub>2</sub> powder, and natural UO<sub>2</sub> powder respectively.

### 요 약

수동적 감마선분석에 의해 U-235의 농축도를 비파괴적으로 측정하였다. 측정대상이 되는 선원은 U-235의 알파붕괴시 방출되는 185.7keV 감마선이다. 농축도 측정에 영향을 미치는 인자, 즉 시료구성, 시료용기의 두께 변화에 따른 감쇠효과, 감마선의 집속 및 검출효율 등을 평가하였다. 최적계측시스템하에서 측정된 상대오차는 95% 신뢰구간에서 Tag값과 비교했을 때 감손 UF<sub>6</sub> 실린더에 대해서는 ~8%, 감손 및 천연 UO<sub>2</sub> 분말에 대해서는 ~8%, ~1%로 각각 나타났다.

### 1. Introduction

In accordance with the obligation required under Korea-IAEA Agreements,<sup>1)</sup> all nuclear materials in bulk facilities and item facilities have to be accounted for and controlled on the basis of

measurement by users. In implementation of the agreements users are also required to establish measurement system in each facility, in which chemical analysis, non-destructive analysis, weighing and volume measurement may be included.

The selection of measurement method usually

depends on the characteristics of sample. Non-destructive assay (NDA) method, for example, is applied when nuclear materials to be measured are distributed irregularly within solid and liquid wastes, when sampling for chemical analysis is not possible on final products like bundles and assemblies, and finally for continuous process line where the accuracy is not important but the qualitative verification is useful.

One other thing to be seriously considered is that inspection should be carried out effectively minimizing interferences on normal plant operation as far as possible.

Gamma-ray analysis is one of NDA method which may be effectively applied for U-235 enrichment measurement, and Pu isotope measurement in sample.

In this paper, the method of enrichment measurement of nuclear materials by passive gamma-ray analysis has been established. For the measurement of U-235 isotope contents in nuclear materials, various instrumental parameters which depend on the type and composition of measured sample materials were independently adjusted to give an optimized measured condition. Under the that condition gamma-ray of U-235 isotope was measured and analyzed to relate it to the isotopic enrichment of unknown uranium samples.

## 2. Theoretical Background

The enrichment measurement is based on the fact that 185.7keV gamma activity is proportional to U-235 contents in uranium sample.<sup>2)-4)</sup> The gamma-ray is heavily attenuated by high density uranium element itself with mass attenuation coefficient<sup>5)</sup> of  $1.5 \text{ cm}^2/\text{g}$  which is about 12 times greater than elements below atomic number  $Z=30$  ( $\mu_m=0.13 \text{ cm}^2/\text{g}$ ). Thus the majority of gamma flux viewed by detector comes from the thin surface of uranium sample<sup>6)</sup>. To a very good approx-

imation the sample thickness must be thicker than infinitive thickness  $X_0$ <sup>2)</sup>, where infinitive thickness is defined to be that thickness of material which produces 99% of the measured 185.7 keV gamma-ray activity. Table 1 shows the calculated thickness of various uranium sample materials.

A measurement of this 185.7keV gamma activity with a suitable detector, therefore, forms the basis for an enrichment measurement technique.<sup>2),4)</sup>

Providing that uranium and matrix material are uniformly distributed, the basic measurement configuration is shown in Fig.1.

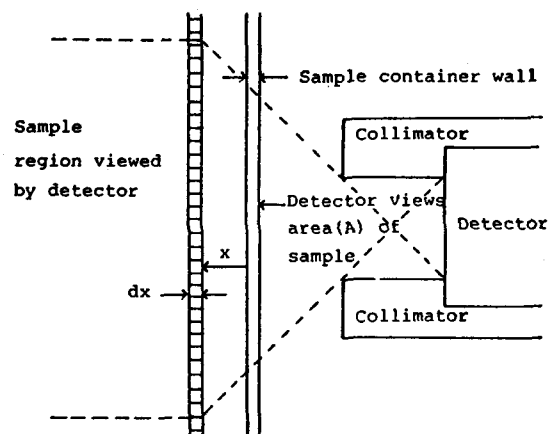


Fig.1 Detector Configuration for Enrichment Measurement

The change of 185.7keV gamma activity  $dC(x)$  (counts/sec) can be expressed in terms of infinitesimal changes at distance  $x$  from sample container wall ;

$$dC(x) = Ea \rho_u A \frac{\Omega}{4\pi} \epsilon \exp \{ (-\rho_u \mu_u - \sum_i \rho_i \mu_i) x \} \exp(-\rho_c \mu_c d) dx \quad (1)$$

where

$E$  = U-235 enrichment ( $\leq 1$ )

$a$  = absolute activity ( $4.3 \times 10^4$  gamma/g.sec)

$\rho$  = density (g/cm<sup>3</sup>)

$u$  : U-235  
 $i$  : matrix material  
 $c$  : container wall

**Table 1. Calculated Values of the Thickness of Material Required to Produce 99% of the Measured 185.7 keV Gamma-ray Activity and Material Composition of Common Fuel Cycle Materials.**

Material	Density <sup>6)</sup> (g/cm <sup>3</sup> )	Infinite thickness <sup>5)</sup> (X <sub>0</sub> ) (cm)	Infinite thickness (X <sub>0</sub> ) (in.)	Material composition term <sup>2)</sup> $(1 + \sum_i \frac{\rho_i \mu_i}{\rho_u \mu_u})$
U(metal)	18.8	0.17	0.067	1.000
UF <sub>6</sub>	4.7	0.94	0.37	1.040
UO <sub>2</sub>	10.9	0.32	0.13	1.012
U <sub>3</sub> O <sub>8</sub>	7.3	0.49	0.19	1.015
Uranyl Nitrate	2.8	2.0	0.79	1.095

$\mu$  = mass attenuation coefficient (cm<sup>2</sup>/g)

$\epsilon$  = absolute efficiency of detector ( $\leq 1$ )

$\frac{\Omega}{4\pi}$  = solid angle ( $\Omega \leq 2\pi$ )

A = sample area defined by collimator (cm<sup>2</sup>)

d = container wall thickness (cm)

The combined count rate from all the material viewed by the detector from x=0 to x=L is therefore given by ;

$$\begin{aligned}
 C &= \int_0^L dC(x) \\
 &= E a \rho_u A \frac{\Omega}{4\pi} \epsilon \exp(-\rho_c \mu_c d) \\
 &\quad \times \int_0^L \exp(-\rho_u \mu_u - \sum_i \rho_i \mu_i) x dx \\
 &= E a \rho_u A \frac{\Omega}{4\pi} \epsilon \exp(-\rho_c \mu_c d) \\
 &\quad \times \left[ \frac{1}{\rho_u \mu_u + \sum_i \rho_i \mu_i} \times \right. \\
 &\quad \left. \{ \exp(-\rho_u \mu_u - \sum_i \rho_i \mu_i) L - 1 \} \right] \quad (2)
 \end{aligned}$$

If length L is taken to be a depth within the sample such that most of the 185.7keV gamma-rays generated at that depth are absorbed before reaching the surface, then  $\exp(-\rho_u \mu_u - \sum_i \rho_i \mu_i) L < 1$ . So the Eq.(2) results in

$$C \approx E \left( \frac{a}{\mu_u} \right) \frac{\Omega A \epsilon}{4\pi} \left[ 1 + \sum_i \frac{\rho_i \mu_i}{\rho_u \mu_u} \right]^{-1}$$

$$\times \exp(-\rho_c \mu_c d) \quad (3)$$

As a result the equation is expressed by 4 different group factors, such as constant, detector efficiency and collimator, sample composition and container wall thickness, and can be calibrated or evaluated independently.<sup>2)</sup>

The measured count rate and the enrichment depend on the composition and homogeneity of the sample, the container wall effect, the detector efficiency, the stability of the detector during the measurements, the background, and counting time.

The count rate is obtained by low energy gamma detection system like 0.5"×3" NaI(Tl) or HPGe directly from UF<sub>6</sub> cylinders, UO<sub>2</sub> powder drums, U metal slab and rods.<sup>7)-10)</sup>

### 3. Experiments

In order to obtain the proper pulses from uranium sample in the detection system the energy calibration has been done first in energy range from 59 keV of <sup>241</sup>Am to 661.6 keV of <sup>137</sup>Cs escape peak with built-in software called "Spectran-AT" of Canberra, U.S.A.

The resulting graph showed the good linearity within useable energy range. The 185.7 keV uranium peak was located at about channel 1119

with HPGe detector (active volume 95.04cm<sup>3</sup>, closed ended coaxial geometry: CANBERRA model GC 2020) (Fig.2).

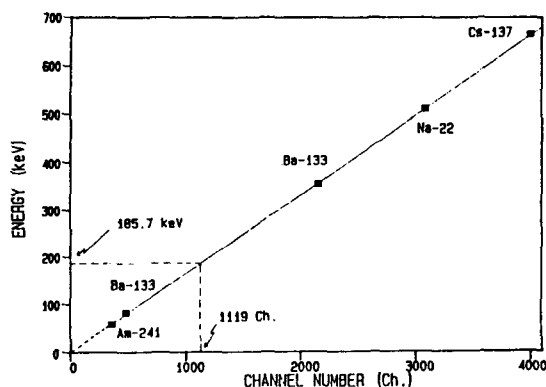


Fig.2 Energy Calibration Curve

#### A. Relationship of Count Rates and Source -to-Detector Distance

In general the count rate obtained from a point gamma source in a detection system is inversely

proportional to source to detector distance, and it is also influenced by detector dead time due to ability of instrument to accept input pulses.<sup>11)</sup>

Table 2 represents the relations of source to detector distance vs collimator. It is outcome of measured count rate of 185.7 keV peak of natural uranium which is 20.5cm diameter by 7.9cm thick and 50.4 kg weight as a standard with and without collimator. In the case of using a suitable collimator the count rate was relatively constant in the corresponding ranges with the half of % dead time.

With reduced % dead time correction due to collimation the measurement was performed at various source to detector distance to find the optimum distance for the particular counting system. The optimum distance was found to be 1/3 of plateau in Fig.3, that was about 4.7cm.

In simple geometrical expression the relationship between the sample area viewed by detector and the detector face could be formulated with variable collimation length (Fig.4). When the

Table 2. Relations of Source to Detector Distance ve Collimator

Without Collimator			With Collimator		
S-D distance (cm)	count rates (c/s)	dead time (%)	S-D distance (cm)	count rates (c/s)	dead time (%)
0.7	567.7 ± 27.9	81.77	2.7	147.4 ± 10.6	34.78
1.7	531.1 ± 20.2	77.32	3.7	146.9 ± 10.6	33.70
2.7	505.1 ± 19.7	73.45	4.7	147.6 ± 10.6	33.33
3.7	476.3 ± 19.1	69.85	5.7	149.0 ± 10.7	32.58
4.7	441.6 ± 18.4	65.42	6.7	149.1 ± 10.7	31.82
5.7	407.1 ± 17.7	61.54	7.7	148.0 ± 10.7	31.03
6.7	377.1 ± 17.0	57.45	8.7	147.3 ± 10.6	30.23
7.7	342.1 ± 16.2	53.67	9.7	146.2 ± 10.6	28.99
			10.7	146.2 ± 10.6	28.14
			11.8	142.1 ± 10.5	26.83
			12.7	136.4 ± 10.2	25.00
			13.7	128.6 ± 9.9	23.57
			14.7	14.7 ± 9.7	22.58

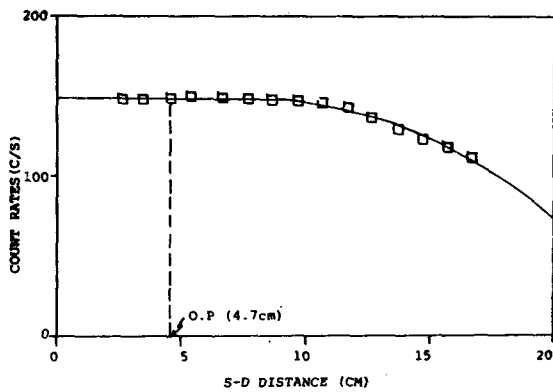


Fig.3 Relation of Count Rates and Source to Detector Distance

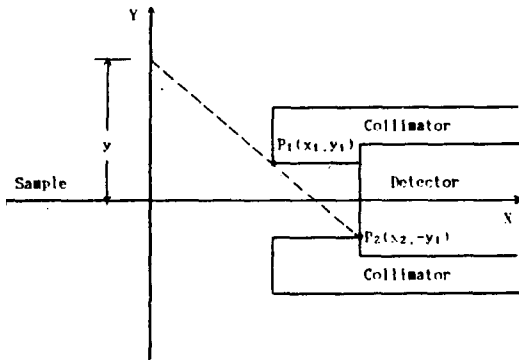


Fig.4 Diagram of Sample Area Measurement Geometry

sample surface area is called  $\pi y^2$  the following equation can be derived ;

$$y = \left( \frac{2y_1}{x_2 - x_1} \right) x_1 + y_1 \tag{4}$$

where

$x_1$  = source to collimator distance (cm)

$x_2$  = source to detector distance (cm)

$y_1$  = collimator radius (cm)

If collimator radius and source to detector distance become fixed, the sample surface area or solid angle is directly dependent on source to collimator face distance.

Thus the experimental measurement for this system resulted in 2.6cm of collimator length, 4.7cm of source to detector distance, and 123.7cm<sup>2</sup> of

sample surface area.

### B. Measurement of Detector Efficiency

If uranium sample is pure metal and outside the container, the equation (3) can be simplified as follows ;

$$C(\text{counts/sec}) = EA \epsilon \left( \frac{\Omega}{4\pi} \right) 2.8 \times 10^4 \text{ gamma/sec.cm}^2 \tag{5}$$

where

$E$  = U-235 enrichment ( $\leq 1$ )

$A$  = sample area viewed through the collimator (cm<sup>2</sup>)

$\frac{\epsilon \Omega}{4\pi} [= \epsilon_i]$  = overall efficiency ( $\leq 1$ )

The counting efficiency ( $\epsilon$ ) and solid angle ( $\Omega/4\pi$ ) term could be treated as one term ( $\epsilon_i$ ) because the length of collimator and source to detector distance were fixed, that is, the sample surface area was determined. In order to determine the overall efficiency the natural U-metal ingot (U-235 isotope 0.7196%) was used for standard sample. As a result of measurement the value of the overall efficiency was decided to be  $5.912 \times 10^{-1}\%$

### C. Container Wall Effect

The gamma flux from uranium source is attenuated by container wall material. The containers for UO<sub>2</sub> powder and UF<sub>6</sub> cylinder are made of steel.<sup>12)</sup>

The mass attenuation coefficient for container wall ( $\mu_c$ ) in Eq.(3) was experimentally determined with accurately known thickness of steel plates (Fig.5).

From Fig.5, the slope of count rate vs various thickness of standard steel could be evaluated by the following equation with the assumption of the assuming back scattering effect=1 ;

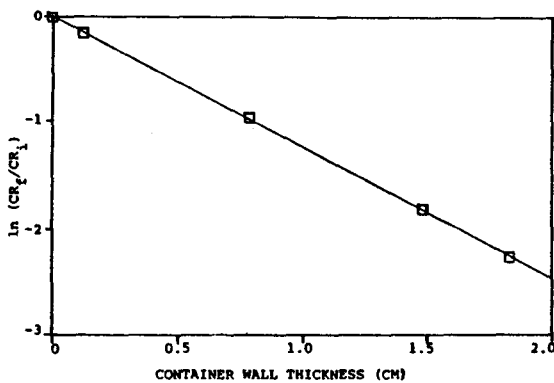


Fig. 5 Relation of Count Rates vs Container Wall Thickness

$$\ln \frac{CR_f}{CR_i} = -\mu_t d = -1.233 \times d \quad (6)$$

$$\text{Slope} = -\mu_t = -1.233 \quad (7)$$

$$\mu_c = \frac{\mu_t}{\rho} \quad (8)$$

where

$CR_i, CR_f$  = initial and final count rate at specified thickness of carbon steel

$\mu_t$  = linear attenuation coefficient ( $\text{cm}^{-1}$ )

$d$  = container wall thickness (cm)

$\mu_c$  = container wall mass attenuation coefficient ( $\text{cm}^2/\text{g}$ )

$\rho$  = density ( $7.8 \text{g}/\text{cm}^3$ )

The value of  $\mu_c$  measured by experiment was found to be  $0.1581 \text{cm}^2/\text{g}$ , whereas the value of  $\mu_c$  quoted by handbook<sup>7)</sup> turn out to be  $0.1603 \text{cm}^2/\text{g}$ .

The measured thickness of the actual cylinder and drum walls, with ultrasonic thickness gauge, were found to be  $1.61 \text{cm}$  and  $0.12 \text{cm}$ , in the average value, respectively. The uncertainty in the thickness measurement was about 1.3%.

#### 4. Unknown Measurement

Experimental system for the unknown measure-

ment consists of coaxial HPGe detector, portable 4096 channel MCA (Series 10, CANBERRA), personal computer/Spectran-AT (PS/2, model 50, IBM), ultrasonic thickness gauge (Nova 100-D, NDT), portable tape recorder, lead collimator, and system supporting table.

Measurements were made on 9 reference samples of 48Y type  $\text{UF}_6$  cylinder and 5 reference samples of 55 gal.  $\text{UO}_2$  drum, with different enrichments between depleted and natural, at KAERI site. Each sample was counted in 5 min. and automatically subtracted the background.

A schematic diagram of the field measurement geometry was shown in Fig. 6.

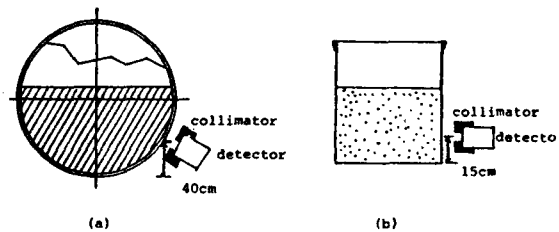


Fig. 6 Schematic Diagram of the Field Measurement Geometry (a)  $\text{UF}_6$  Cylinder and (b)  $\text{UO}_2$  Powder Drum

#### 5. Results and Discussions

A total of 9 each 10 ton  $\text{UF}_6$  cylinders, and 5 each 55 gal. powder drums were randomly selected for experiments. All of them were shipped in from U.S.A. and CANADA accompanied with chemical analysis data.

The raw data obtained from field measurement on samples were analyzed by personal computer with pulse height analysis program purchased through CANBERRA, U.S.A.

The results of measurement on depleted  $\text{UF}_6$  cylinders, depleted and natural  $\text{UO}_2$  powder drums are shown in Table 3,4,5 respectively. Here,  $I_T$  and  $I_M$  represent Tag value and average measured value, respectively, And the relative

**Table 3. Calculated Enrichment of Depleted UF<sub>6</sub> Cylinders**

Cylinder Number	Tag Values (I <sub>T</sub> ) (% U-235)	Average Measured Values at 1.96 σ (I <sub>M</sub> ) (% U-235)	$\frac{I_M - I_T}{I_T} \times 100$ (%)
2	0.2026	0.2125 ± 0.0328	+4.98
3	0.2016	0.2049 ± 0.0294	+1.64
4	0.2016	0.2139 ± 0.0250	+5.37
5	0.2021	0.2048 ± 0.0291	+1.34
6	0.2017	0.2186 ± 0.0310	+8.38
11	0.2020	0.2079 ± 0.0351	+2.92
12	0.2013	0.2006 ± 0.0428	-0.35
14	0.1995	0.2019 ± 0.0154	+1.20
15	0.2020	0.1972 ± 0.0262	-2.38

**Table 4. Calculated Enrichment of Natural UO<sub>2</sub> Powder Drums**

Drum Number	Tag Values (I <sub>T</sub> ) (% U-235)	Average Measured Values at 1.96 σ (I <sub>M</sub> ) (% U-235)	$\frac{I_M - I_T}{I_T} \times 100$ (%)
6	0.7271	0.7337 ± 0.0220	+0.91
11	0.7271	0.7347 ± 0.0094	+1.05
14	0.7271	0.7327 ± 0.0140	+0.77
17	0.7271	0.7261 ± 0.0317	-0.14
19	0.7271	0.7203 ± 0.0108	-0.94

**Table 5. Calculated Enrichment of Depleted UO<sub>2</sub> Powder Drums**

Drum Number	Tag Values (I <sub>T</sub> ) (% U-235)	Average Measured Values at 1.96 σ (I <sub>M</sub> ) (% U-235)	$\frac{I_M - I_T}{I_T} \times 100$ (%)
12	0.21	0.2240 ± 0.0162	+6.67
15	0.21	0.2170 ± 0.0153	+3.33
19	0.21	0.2203 ± 0.0153	+4.90
29	0.21	0.2218 ± 0.0108	+5.62
38	0.21	0.2267 ± 0.0099	+7.95

errors were at 95% confidence level ~8% for cylinders, ~8%, ~1% for depleted and natural drums in comparison with Tag values.

The principal source of the error was found to be the uncertainty arising from the measurement of container wall thickness by ultrasonic thickness gauge (see Eq.(3)).

In reducing the source of errors in over-all counting system the followings are suggested; 1) calibration of ultrasonic gauge with reference material as close as possible to container wall material, 2) to maintain signal amplifier stabilized by prolonged warm-up time, and 3) to allow relatively long counting time.

The limiting conditions for the enrichment measurement were that the composition of sample must be homogeneous and the sample thickness also must be thicker than infinitive thickness.

As for the detector efficiency and collimator factor ( $\epsilon \times \Omega / 4\pi$ ) of Eq.(5), the most idealistic case is that the collimator area equals to sample area by extending collimation up to the surface of bare sample. But most samples can not meet this condition because of the container wall thickness. When source to detector distance and collimator length are fixed allowing sufficient distance for container wall and then solid angle and detector efficiency,  $\epsilon \times \Omega / 4\pi$ , can be considered as one factor, that is, overall efficiency,  $\epsilon_t$ .

### 6. Conclusion

Under the uranium sample's infinitive thickness and homogeneous sample matrix the quantitative measurement of uranium enrichment by passive non-destructive gamma-ray analysis is possible. The accuracy of measurement for uranium enrichment was achieved about ~8% error at 95% confidence level. So the quantitative non-destructive assay method can be applied not only to uranium sample which emits gamma-ray. More specific applications can include the qualitative verification of nuclear materials upon receiving from outside facility the enrichment verification of nuclear fuel elements, the homogeneity test for  $UO_2$  powder in fuel fabrication process, and lastly the measurement of uranium contents in wastes for safeguards accountability purpose.

### References

1. Agreement between Government of the Republic of Korea and IAEA for the Application of Safeguards in Connection with Treaty on the Non-proliferation of Nuclear Weapons, (1975).
2. L.A. Kull and R.O. Ginaven, Guidelines for Gamma-Ray Spectroscopy Measurements of U-235 enrichment, BNL-50414, (1974).
3. M.Takahashi, Regional Training Course on State Systems of Accounting for and Control of Nuclear Material, 4.2, (1985).
4. R.H. Auguston and T.D. Really, Fundamentals of Passive Non-Destructive Assay of Fissionable Material, Los Alamos Scientific Laboratory, LA-5651-M, Sept.,(1974).
5. J.H. Hubbel, Photon Cross Section, Attenuation Coefficients and Energy Absorption Coefficients from 10 keV to 100 GeV, N-SRDS-NBS 29, (1969).
6. E.F. Plechaty and J.R. Terral, Photon Cross Sections 1 keV to 100 MeV, TID-4500, (1968).
7. R.Sher, S.Untermyer II, The Detection of Fissionable Materials by Nondestructive Means, American Nuclear Society, (1980).
8. R.B. Walton, T.D. Really, J.L. Parker, J.H. Menzel, E.D. Marshall, and L.W. Fields, Measurement of  $UF_6$  cylinders with Portable Instruments, Nucl. Tech, Vol. 21 P 133, (1974).
9. J.H. Hong, 핵물질 계량 기술 개발, KAERI/RR-735, (1988).
10. R.Waldman, Enrichment determinations of Uranium Dioxide Powders and Pellets Using Hyperpure Germanium Detectors in Field Conditions, BLG 634, (1980).
11. C.E. Crouthamel, Applied Gamma-ray Spectrometry, Pergamon Press.
12. Uranium Hexafluoride: Handling Procedures and Container Criteria, ORO-651, (1981).